EUROPEAN JOURNAL OF PURE AND APPLIED MATHEMATICS
2025, Vol. 18, Issue 4, Article Number 6254
ISSN 1307-5543 – ejpam.com
Published by New York Business Global

Mathematical Modeling of SEIRV Epidemic Model With Delay and Optimal Control of Holling Type II

Shumaila Irum[1], Anwar Zeb[1,*], Ahmed A. Mohsen[2,3], Thoraya N. Alharthi[4], Ilyas Khan[5,6,7], Osama Oqilat[8], Wei Sin Koh[9]

[1] *Department of Mathematics, COMSATS University Islamabad, Abbottabad Campus, Pakistan*
[2] *Department of Mathematics, Open Education College, Iraq*
[3] *Department of Mathematics, College of Education for Pure Science (Ibn Al-Haitham), University of Baghdad, Baghdad, Iraq*
[4] *Department of Mathematics, College of Science, University of Bisha, P.O. Box 551, Bisha 61922, Saudi Arabia*
[5] *Department of Mathematical Sciences, Saveetha School of Engineering, SIMATS, Chennai, Tamil Nadu, India*
[6] *Hourani Center for Applied Scientific Research, Al-Ahliyya Amman University, Amman, Jordan*
[7] *Department of Mathematics, College of Science Al-Zulfi, Majmaah University, Al-Majmaah 11952, Saudi Arabia*
[8] *Hourani Center for Applied Scientific Research, Department of Basic Sciences, Faculty of Arts and Science, Al-Ahliyya Amman University, Amman, Jordan*
[9] *INTI International University, Persiaran Perdana BBN Putra Nilai, 71800 Nilai, Negeri Sembilan, Malaysia*

Abstract. This work proposes a mathematical model of the SEIRV epidemic framework incorporating time delays and optimal control strategies based on Holling Type II functional responses. The SEIRV model, which includes compartments for Susceptible, Exposed, Infectious, Recovered, and Vaccinated individuals, is extended to account for delays in the transmission and vaccination processes. The stability and behavior of the model are analyzed using differential equations and delay differential equations. Optimal control technique is applied to minimize the spread of infection and optimize vaccination strategies, considering resource limitations and practical constraints. Numerical simulations demonstrate the effectiveness of the proposed control strategies in reducing infection rates and achieving disease eradication. The findings contribute to the understanding of epidemic dynamics and provide valuable information for public health policy and intervention planning.

2020 Mathematics Subject Classifications: 92D30, 49N90, 34K20

Key Words and Phrases: Diseases, seirv epidemic model, time delay, optimal control

*Corresponding author.
DOI: https://doi.org/10.29020/nybg.ejpam.v18i4.6254

Email addresses: shumaila@cuiatd.edu.pk (S. Irum),
anwar@cuiatd.edu.pk (A. Zeb),
aamuhseen@gmail.com (A. A. Mohsen),
talhrthe@ub.edu.sa (T. N. Alharthi),
i.said@mu.edu.sa (I. Khan),
weisin.koh@newinti.edu.my (W. S. Koh)

1. Introduction

Throughout the last several decades, infectious diseases have posed significant challenges to public health worldwide. Despite advances in medical science, diseases such as malaria and tuberculosis continue to affect millions. Although numerous studies have been conducted on prevention and treatment, a significant knowledge gap persists on the mechanisms of disease spread under varying environmental conditions. This research aims to develop a comprehensive model for predicting infectious disease outbreaks. The study tells us about the influence of climate variations on disease transmission. And also tells the role of human behaviors in spreading infections. This research aims to contribute to the development of more effective disease control strategies. However, this study is limited to data from specific regions and may not be universally applicable. This paper argues that incorporating environmental factors into disease prediction models significantly improves their accuracy.

Mathematical modeling has proven indispensable in understanding and containing infectious diseases. The SEIRV model, which includes compartments for susceptible, exposed, infectious, recovered, and vaccinated individuals, provides a comprehensive framework for studying disease dynamics. These models were also used during the COVID-19 pandemic [1–6]. The classical SEIR (Susceptible–Exposed–Infectious–Recovered) model has been widely used to study the dynamics of infectious diseases. However, the emergence of vaccination as a pivotal public health strategy necessitates the inclusion of a Vaccinated (V) compartment, resulting in the extended SEIRV framework. The motivation for this work stems from the need to understand how vaccination policies influence disease spread, especially in realistic settings that involve time delays, control strategies, and nonlinear incidence rates. The novelty of this study lies in incorporating a time-delayed transmission dynamic and an optimal control approach in the SEIRV model, enabling the analysis of how delays in exposure or treatment impact epidemic control. Furthermore, the model accommodates a Holling Type II incidence function, which better captures the saturation effects in disease transmission, reflecting the limitations of the behavioral and medical response. This extended SEIRV model is applicable to the evaluation and design of effective vaccination campaigns and public health interventions during outbreaks such as COVID-19, measles, or influenza. It can assist policymakers in determining optimal resource allocation for vaccination and treatment, timing of intervention strategies, and understanding the long-term impact of delayed responses. The model is particularly relevant for guiding decision making in regions with constrained healthcare infrastructure and variable public response [7, 8]. However, existing models often overlook the impact of delays and optimal control mechanisms. This study aims to develop and analyze a delayed SEIRV epidemic model incorporating optimal control with a Holling-type II functional response. By incorporating delays, we seek to understand their effect on disease spread and identify optimal control strategies to mitigate outbreaks. This study addressed how do delays influence the transmission dynamics of the disease and what are the most effective control strategies under different scenarios. The scope of this research is restricted to theoretical analysis and simulations based on specific parameter values. This paper

argues that incorporating delays and optimal control into the SEIRV model significantly enhances its predictive accuracy and effectiveness in disease management.

Mathematical modeling using the SEIRV epidemic framework (especially with its complexities like delays and the quest for optimal control) is far more than an academic exercise. It stands as a guiding light in the global fight against infectious diseases. In exploring this model's depth, we are not merely working with equations or computations but we are developing powerful tools to forecast, manage, and ultimately overcome epidemics.

Diving into the SEIRV epidemic model with delay and Holling type delay optimal control, we are not just working with numbers and equations we are forging advanced tools for public health. This model is not merely theoretical it is a blueprint for predicting and controlling outbreaks, potentially saving countless lives. Stay motivated, as our contributions could well be the key to unlocking the mysteries of infectious disease dynamics. This model helps in understanding the spread and control of infectious diseases through the incorporation of various factors such as susceptible, exposed, infected, recovered, and vaccinated individuals. The delay aspect accounts for the incubation period of the disease, making the model more realistic [9, 10].

After reading the paper [11], we were inspired to extend the research. We observed that incorporating time delay and optimal control had not yet been explored in this context, so we introduced these elements as novel contributions. By applying optimal control theory, the model identifies the most effective strategies to curb the spread of infectious diseases while accounting for resource limitations. This approach is essential for effective public health planning and intervention [12]. To better capture the dynamics between the disease and the population, the model utilizes the Holling Type II functional response, which offers a more realistic depiction of how infections progress and impact the population [13]. The insights gained from this model can aid policymakers in determining optimal strategies for controlling epidemics, such as vaccination, quarantine, and other public health measures [12, 14]. This framework also lays the groundwork for future epidemiological research, enabling scientists to develop innovative approaches for disease prevention and health improvement [9]. Ultimately, studying this model empowers researchers to contribute significantly to efforts aimed at controlling and preventing the spread of infectious diseases, thereby saving lives and enhancing public health outcomes [12].

This paper is structured as follows: In Section 2, we introduce the mathematical model with time delay and its solution. In Section 3, we formulate the mathematical epidemic model SEIRV with optimal control and its solution are find. In Section 4, we provide a numerical method alongside the relevant simulation results. In summery, Section 5 compiles the final conclusion and discussion.

2. Formulation of SEIRV Model with Time Delay

In this paper, we consider the model presented in [11], which was discussed without delay and optimal control. In their model, they have divided the total population $N(t)$ at time $t > 0$ into five compartments. These are $S(t)$ susceptible populations that are at risk of infection but have not been exposed to the infected yet, exposed $E(t)$ de-

notes the exposed population that has come into contact with the infected people but is not infectious. These people are in a latent state, $I(t)$ refers to infectious people that spread the infection to other people, $R(t)$ indicates recovered people who are no longer infected by the infection. ,and $V(t)$ stands for the vaccinated population. Therefore $N(t)$=S(t)+E(t)+$I(t)$+$R(t)$+$V(t)$. Each compartment presents a unique scenarios.For example the population of $S(t)$ compartment increased by recruitment rate Δ and passed away naturally at a rate of μ, vaccination at a rate of γ_2 and transmission at a rate of β with term $\frac{\beta SI}{1+\alpha I}$, where α being the saturated rate.The population of $E(t)$ compartment passed away naturally at a rate of μ, with latency period σ . The population of $I(t)$ compartment decreased by natural death at a rate of μ, with speed of recovery rate γ_1 . The population of the $R(t)$ compartment decreased of natural causes at a rate of μ, and vaccinated at a rate of γ_3. Similarly, the population of the $V(t)$ compartment passed away naturally at a rate of μ. However, delay and optimal control play a crucial role in the dynamics of epidemic models. Therefore, in this study, we investigate a system of differential equations incorporating time delays to capture these essential effects more accurately. Here $\tau > 0$ represents the response time of disease, which follows a similar argument in [15, 16] in the model presented in [11]. The model is as follows for the SEIRV framework.

$$\begin{aligned}
\frac{dS(t)}{dt} &= \Delta - \frac{\beta S(t)I(t)}{1+\alpha I(t)} - \mu S(t) - \gamma_2 S(t),\\
\frac{dE(t)}{dt} &= \frac{\beta S(t)I(t)}{1+\alpha I(t)} - \sigma E(t-\tau) - \mu E(t),\\
\frac{dI(t)}{dt} &= \sigma E(t-\tau) - \gamma_1 I(t) - \mu I(t),\\
\frac{dR(t)}{dt} &= \gamma_1 I(t) - \gamma_3 R(t) - \mu R(t),\\
\frac{dV(t)}{dt} &= \gamma_2 S(t) + \gamma_3 R(t) - \mu V(t).
\end{aligned} \tag{1}$$

The initial conditions of the above system as follows:

$$\begin{cases} S(0) = S(\theta) > 0, E(0) = E(\theta) \geq 0, I(0) = I(\theta) \geq 0, \\ R(0) = R(\theta) \geq 0, V(0) = V(\theta) \geq 0, \end{cases} \tag{2}$$

where, $\theta \in [-\tau, 0]$ is assumed. The proposed model has two equilibrium points that are disease-free equilibrium point:
$E_0(S_0.E_0, I_0, R_0, V_0) = E_0(\frac{\Lambda}{\mu+\gamma_2}, 0, 0, 0, \frac{\gamma_2\Lambda}{\mu(\mu+\gamma_2)})$,
and endemic equilibrium point:
$E_*(S_*.E_*, I_*, R_*, V_*) = E_*(\frac{(\sigma+\mu)(\gamma_1+\mu)(1+\alpha I_*)}{\beta\sigma}, \frac{(\gamma_1+\mu)(\gamma_2+\mu)(R_0-1)}{\sigma(\beta+\alpha(\mu+\gamma_2))}, \frac{(\mu+\gamma_2)(R_0-1)}{\beta+\alpha(\mu+\gamma_2)}, \frac{\gamma_1(R_0-1)}{\beta+\alpha(\mu+\gamma_2)}, \frac{\gamma_2(S_*+R_*)}{\mu})$.
Reproductive number is give as:
$R_0 = \frac{\beta\Lambda\sigma}{(\sigma+\mu)(\gamma_1+\mu)(\gamma_2+\mu)}$.
On the same way, the first three equations of system (1) are independent of fourth and fifth variables R and V, enabling us to analyze the system by examining the subsystem,

as

$$\begin{aligned}
\frac{dS(t)}{dt} &= \Delta - \frac{\beta S(t)I(t)}{1+\alpha I(t)} - \mu S(t) - \gamma_2 S(t),\\
\frac{dE(t)}{dt} &= \frac{\beta S(t)I(t)}{1+\alpha I(t)} - \sigma E(t-\tau) - \mu E(t),\\
\frac{dI(t)}{dt} &= \sigma E(t-\tau) - \gamma_1 I(t) - \mu I(t).
\end{aligned} \tag{3}$$

Theorem 1. *The solutions of system (3) remain bounded and non-negative for all time $t \geq 0$, provided that the initial conditions are non-negative. That is, every solution remains in a positively invariant set $\Omega \subset \mathbb{R}^3_+$, and $(S(t), E(t), I(t)) \in \mathbb{R}^3_+$ for all $t \geq 0$.*

Proof. Suppose $N(t)$=S(t)+E(t)+$I(t)$, then

$$\begin{aligned}
\frac{dN}{dt} &= \frac{d}{dt}(S(t)) + \frac{d}{dt}(E(t)) + \frac{d}{dt}(I(t)),\\
\frac{dN}{dt} &= \Delta - \mu\left(S(t)+E(t)+I(t)\right) - \gamma_2 S(t) - \gamma_1 I(t),\\
\frac{dN(t)}{dt} &= \Delta - \mu N(t) - \gamma_2 S(t) - \gamma_1 I(t) \leq \Delta - \mu N(t),\\
\frac{d}{dt}\left(Ne^{\mu t}\right) &\leq \Delta e^{\mu t},
\end{aligned}$$

implies that

$$N(t) \leq \frac{\Delta}{\mu} + \mathbb{B}e^{-\mu(t)}.$$

Thus,

$$0 \leq N(t) \leq \frac{\Delta}{\mu} \quad \text{as} \quad t \to \infty.$$

Consequently, the dynamic of the model can be analyzed within the region:

$$\Omega = \{(S(t), E(t), I(t)) \in \mathbb{R}^3_+ : N \leq \frac{\Delta}{\mu}\},$$

then the set Ω is positive invariant with respect system (3) and hence it is closed.

2.1. Linearization

To linearized the system (3), we apply Taylor series. For simplicity, we represent this process as follows:

$$\frac{dS}{dt} = f(S(t), E(t), I(t)),$$

where

$$f(S(t), E(t), I(t)) = \Delta - \frac{\beta S(t)I(t)}{1+\alpha I(t)} - \mu S(t) - \gamma_2 S(t)$$

$$\frac{dE}{dt} = g(S(t), E(t), I(t)),$$

where

$$g(S(t), E(t), I(t)) = \frac{\beta S(t) I(t)}{1 + \alpha I(t)} - \sigma E(t - \tau) - \mu E(t)$$

$$\frac{dI}{dt} = h(S(t), E(t), I(t))$$

where

$$h(S(t), E(t), I(t)) = \sigma E(t - \tau) - \gamma_1 I(t) - \mu I(t).$$

We define
$S - S_* = u, \quad E - E_* = v, \quad I - I_* = w.$
Now expansion of model (3) around the point (S_*, E_*, I_*) is given by:

$$\dot{u} = u\left(-\frac{\beta I_*}{1 + \alpha I_*} - \mu - \gamma_2\right) + v(0) + w\left(-\frac{\beta S_*}{(1 + \alpha I_*)^2}\right),$$

similarly

$$\begin{aligned} \dot{v} &= u\left(\frac{\beta I_*}{1 + \alpha I_*} -\right) + v(-\mu - \sigma e^{-\lambda\tau}) + w\left(\frac{\beta S_*}{(1 + \alpha I_*)^2}\right), \\ \dot{w} &= u(0) + v(-\sigma)e^{-\lambda\tau} + w(-\mu - \gamma_1). \end{aligned}$$

2.2. Matrix Representation of the Linearized System

The linearized system for (3) is expressed in matrix form as follows:

$$\begin{pmatrix} \dot{u} \\ \dot{v} \\ \dot{w} \end{pmatrix} = \begin{pmatrix} \frac{\partial f}{\partial S} & \frac{\partial f}{\partial E} & \frac{\partial f}{\partial I} \\ \frac{\partial g}{\partial S} & \frac{\partial g}{\partial E} & \frac{\partial g}{\partial I} \\ \frac{\partial h}{\partial S} & \frac{\partial h}{\partial E} & \frac{\partial g}{\partial I} \end{pmatrix} \begin{pmatrix} u \\ v \\ w \end{pmatrix}.$$

Alternatively, in simplified notation:

$$\dot{X} = JX,$$

where J represents the Jacobian matrix, composed of the derivatives of each term on the right-hand side of the model's equations, namely (S, E, I). So, with linearization the system obtains the following form:

$$\begin{cases} \frac{du}{dt} &= a_{11}u + a_{13}w, \\ \frac{dv}{dt} &= a_{21}u + ua_{22}v + b_{22}u\big(t - \tau\big) + a_{23}w, \\ \frac{dw}{dt} &= b_{32}v\big(t - \tau\big) + a_{33}w, \end{cases} \tag{4}$$

where

$$\begin{aligned} a_{11} &= -\frac{\beta I_*}{1 + \alpha I_*} - \mu - \gamma_2, \\ a_{13} &= -\frac{\beta S_*}{(1 + \alpha I_*)^2}, \\ a_{21} &= \frac{\beta I_*}{1 + \alpha I_*} - \mu - \gamma_2, \end{aligned}$$

$$\begin{aligned} a_{22} &= -\mu, \\ a_{23} &= \frac{\beta S_*}{(1+\alpha I_*)^2}, \\ a_{33} &= -\gamma_1 - \mu, \\ b_{22} &= -\sigma \\ b_{32} &= \sigma. \end{aligned}$$

Thus, the Jacobian of system (4) is

$$J = \begin{bmatrix} a_{11} & 0 & a_{13} \\ a_{21} & a_{22} + b_{22}e^{-\lambda\tau} & a_{23} \\ 0 & b_{32}e^{-\lambda\tau} & a_{33} \end{bmatrix}.$$

For eigen values, solve $|\lambda I - J| = 0$,

$$\begin{vmatrix} \lambda - a_{11} & 0 & -a_{13} \\ -a_{21} & \lambda - (a_{22} + b_{22}e^{-\lambda\tau}) & -a_{23} \\ 0 & -b_{32}e^{-\lambda\tau} & \lambda - a_{33} \end{vmatrix} = 0.$$

After solving the determinant we acquire the characteristic equation:

$$\lambda^3 + p_1\lambda^2 + p_2\lambda + p_3 + \left(q_1\lambda^2 + q_2\lambda + q_3\right)e^{-\lambda\tau} = 0. \tag{5}$$

Here

$$\begin{aligned} p_1 &= -a_{11} + a_{22} + a_{33}, \\ p_2 &= a_{11}a_{22} + a_{11}a_{33} + a_{22}a_{33}, \\ p_3 &= -a_{11}a_{22}a_{33}, \\ q_1 &= -b_{22}, \\ q_2 &= a_{33}b_{22} - a_{23}b_{32} + a_{11}b_{22}, \\ q_3 &= a_{13}a_{23}b_{32} + a_{13}a_{22}b_{32}d_6 - a_{11}b_{22}a_{33} \end{aligned}$$

When $\tau = 0$, then

$$\lambda^3 + (p_1 + q_1)\lambda^2 + (p_2 + q_2)\lambda + (p_3 + q_3) = 0. \tag{6}$$

Let suppose:

$$\begin{aligned} D_2 &= p_1 + q_1, \\ D_1 &= p_2 + q_2, \\ D_0 &= p_3 + q_3. \end{aligned}$$

Equation (6) become:

$$\lambda^3 + D_2\lambda^2 + D_1\lambda + D_0 = 0. \tag{7}$$

By using the Hurwitz criteria, E_* exhibits local asymptotic stability at $\tau = 0$, under the following conditions:

$$det_1 = D_2 > 0, \tag{8}$$

$$det_2 = \begin{pmatrix} D_2 & 1 \\ D_0 & D_1 \end{pmatrix} > 0, \tag{9}$$

$$det_3 = \begin{pmatrix} D_2 & 1 & 0 \\ D_0 & D_1 & D_2 \\ 0 & 0 & D_0 \end{pmatrix} > 0. \tag{10}$$

Since the model parameters are all positive, then it is always asymptotically stable, which shows all roots lie on the left half plane.

In the same way, when $\tau > 0$, we consider the characteristics equation provided in eq (5) and, setting $\lambda = \iota\omega$, we have

$$\lambda^3 + p_1\lambda^2 + p_2\lambda + p_3 + \left(q_1\lambda^2 + q_2\lambda + q_3\right) e^{-\iota\omega\tau} = 0. \tag{11}$$

By separated the real and imaginary parts of above equation we have

$$\begin{aligned} (q_3 - q_1\omega^2)\cos(\omega\tau) + q_2\omega\sin(\omega\tau) &= p_1\omega^2 - p_3, & (12)\\ q_2\omega\cos(\omega\tau) - (q_3 - q_1\omega^2)\sin(\omega\tau) &= \omega^3 - p_2\omega & (13) \end{aligned}$$

which leads to

$$\omega^6 + \left(p_1^2 + 2p_2 - q_1^2\right)\omega^4 + (p_2^2 - 2p_1p_3 - q_2^2 + 2q_1q_3)\omega^2 + (p_3^2 + q_3^2) = 0. \tag{14}$$

If $t = \omega^2$, then above equation becomes

$$t^3 + s_1t^2 + s_2t + s_3 = 0. \tag{15}$$

where

$$\begin{cases} s_1 &= \left(p_1^2 + 2p_2 - q_1^2\right), \\ s_2 &= (p_2^2 - 2p_1p_3 - q_2^2 + 2q_1q_3), \\ s_3 &= (p_3^2 + q_3^2), \end{cases}$$

Thus by substituting s_1, s_2, s_3 in above equation, we have negative roots which implies that it is asymptotically stable.

3. Epidemic Model SEIRV-Formulation with optimal control

In this section, we examine control strategy of model model presented in [11]. The population of $E(t)$ reduced with control u_1 as quarantine. The population of $I(t)$ compartment decreased with control u_2 as treatment . The population of the $R(t)$ compartment is increased by control u_1 of the exposed class and cotrol u_2 of infected class.

Thus the optimal control model can be expressed as:

$$\begin{aligned}
\frac{dS(t)}{dt} &= \Delta - \frac{\beta S(t)I(t)}{1+\alpha I(t)} - \mu S(t) - \gamma_2 S(t),\\
\frac{dE(t)}{dt} &= \frac{\beta S(t)I(t)}{1+\alpha I(t)} - \sigma E(t) - \mu E(t) - u_1 E(t),\\
\frac{dI(t)}{dt} &= \sigma E(t) - \gamma_1 I(t) - \mu I(t) - u_2 I(t),\\
\frac{dR(t)}{dt} &= \gamma_1 I(t) - \gamma_3 R(t) - \mu R(t) + u_1 E(t) + u_2 I(t),\\
\frac{dV(t)}{dt} &= \gamma_2 S(t) + \gamma_3 R(t) - \mu V(t).
\end{aligned} \tag{16}$$

Our aim to decrease the number of Exposed and Infected individuals while increase the count of recovering throughout the epidemic. Mathematically, for a fixed terminal time t_i, the problem is to minimize the objective function, which is given as:

$$\mathbb{J}(u_1,u_2) = \int_0^T \left[A_1 S(t) + A_2 E(t) + A_3 I(t) - A_4 R(t) + A_5 V(t) + \frac{A_6}{2}u_1^2(t) + \frac{A_7}{2}u_2^2\right] dt. \tag{17}$$

In the above expression, $A_i \geq 0$ (for $i = 1..7$) represents the scaling factors that adjust the contribution of each term in the functional. The objective is to find the optimal control pairs u_1^*,u_2^* such that:

$$\mathbb{J}(u_1^*, u_2^*) = \min\{\mathbb{J}(u_1,u_2) : u_1, u_2 \in \mathbb{U}\}. \tag{18}$$

In this setting, $\mathbb{U}$ denotes the pair of feasible controls, given by:

$$\mathbb{U} = \{u = u_i(t) : 0 \leq u_i(t) \leq u_i^{\max} \leq 1,\, t \in [0,T], i = 1,2\}. \tag{19}$$

Here u is Lebesgue measurable.
The flow chart of the model (16) is presented in Fig. (1).

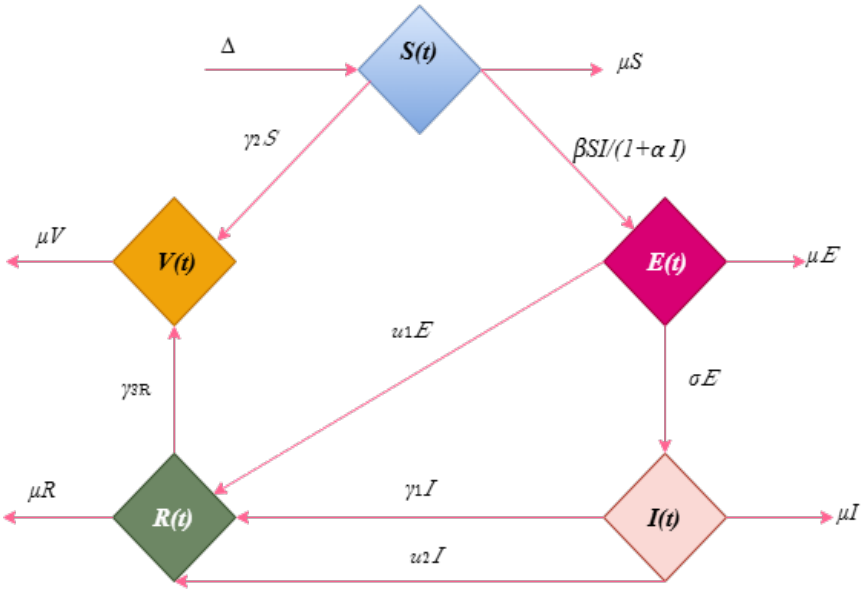

Figure 1: Flow chart of model (16)

Now, we first find the kernels of control model. For this purpose, we introduce the functions K_i where $i \in \{1, \ldots, 5\}$, while assuming $L[0, 1]$. We describe these functions in the following manner:

$$
\begin{aligned}
K_1(t, S) &= \Delta - \frac{\beta S(t) I(t)}{1 + \alpha I(t)} - (\gamma_2 + \mu) S(t), \\
K_2(t, E) &= \frac{\beta S(t) I(t)}{1 + \alpha I(t)} - (\sigma + \mu) E(t) - u_1 E(t), \\
K_3(t, I) &= \sigma E(t) - (\gamma_1 + \mu) I(t) - u_2 I(t) \\
K_4(t, R) &= \gamma_1 I(t) - \gamma_3 R(t) - \mu R(t) + u_1 E(t) + u_2 I(t), \\
K_5(t, V) &= \gamma_2 S(t) + \gamma_3 R(t) - \mu V(t)
\end{aligned}
$$

Theorem 2. *Given the assumptions stated above, the kernels K_i satisfy the Lipschitz condition and are contractions if and only if the Lipschitz constants $\psi_j < 1$ where $j \in \{1, \ldots, 5\}$, for each $i \in \{1, \ldots, 5\}$.*

Proof. For proof of this theorem we are employing certain conditions on the kernels:
Lipschitz Condition for $K_1(S)$:

$$
\begin{aligned}
\|K_1(S) - K_1(S^*)\| = \Bigg\| & \Delta - \frac{\beta S I}{1 + \alpha I} - (\gamma_2 + \mu) S \\
& - \left(\Delta - \frac{\beta S^* I}{1 + \alpha I} - (\gamma_2 + \mu) S^* \right) \Bigg\|, \\
\leq & \left\| \frac{\beta I}{1 + \alpha I + (\gamma_2 + \mu)} \right\| \|S - S^*\|, \\
= & \, \psi_1 \|S - S^*\|,
\end{aligned}
$$

where

$$\psi_1 = \left\| \frac{\beta I}{1 + \alpha I + (\gamma_2 + \mu)} \right\|.$$

Lipschitz Condition for $K_2(E)$:

$$\begin{aligned} \|K_2(E) - K_2(E^*)\| &= \left\| \frac{\beta SI}{1+\alpha I} - (\sigma+\mu)E - u_1 E \right. \\ &\quad \left. - \left[\frac{\beta SI}{1+\alpha I} - (\sigma+\mu)E^* - u_1 E^* \right] \right\|, \\ &\leq \left\| \frac{\beta SI}{1+\alpha I} + (\sigma+\mu) + u_1 \right\| \|E - E^*\|, \\ &= \psi_2 \|E - E^*\|, \end{aligned}$$

where

$$\psi_2 = \left\| \frac{\beta SI}{1+\alpha I} + (\sigma+\mu) + u_1 \right\|.$$

Lipschitz Condition for $K_3(I)$:

$$\begin{aligned} \|K_3(I) - K_3(I^*)\| &= \|\sigma E - (\gamma_1+\mu)I - u_2 I - [\sigma E - (\gamma_1+\mu)I^* - u_2 I^*]\|, \\ &\leq \|(\gamma_1+\mu) + u_2\| \, \|I - I^*\|, \\ &= \psi_3 \|I - I^*\|, \end{aligned}$$

where

$$\psi_3 = \|(\gamma_1+\mu) + u_2\|.$$

Lipschitz Condition for $K_4(R)$:

$$\begin{aligned} \|K_4(R) - K_4(R^*)\| &= \|\gamma_1 I - \mu R + u_1 E + u_2 I - [\gamma_1 I - \mu R^* + u_1 E + u_2 I]\|, \\ &\leq \|\mu\| \, \|R - R^*\|, \\ &= \psi_3 \|R - R^*\|, \end{aligned}$$

where

$$\psi_4 = \|\mu\|.$$

Lipschitz Condition for $K_5(V)$:

$$\begin{aligned} \|K_5(V) - K_5(V^*)\| &= \|\gamma_2 S - \gamma_3 R - \mu V - [\gamma_2 S - \gamma_3 R - \mu V^*]\|, \\ &\leq \|\mu\| \, \|V - V^*\|, \\ &= \psi_5 \|V - V^*\|, \end{aligned}$$

where

$$\psi_5 = \|\mu\|.$$

Therefore, the analysis of the Lipschitz conditions demonstrates that the kernels satisfy the criteria for being contractions.

3.1. Existence of an optimal control pair

This section presents a finding on whether an optimal control exists within the model we proposed.

Theorem 3. *Consider the control problem with the system* (16). *There exists an optimal control pair* $u_i^* \in \mathbb{U}$ *such that:*

$$\mathbb{J}(u_i^*) = \min\{\mathbb{J}(u_i) : u_i \in \mathbb{U}, i = 1, 2\}. \tag{20}$$

Proof. To establish the existence of an optimal control, we utilize a result by Fleming and Rishel [17]. The following conditions are be checked:

(i) The set of controls and the corresponding state variables must be nonempty. The existence of solution for system (16) is proved using result by Lukes [18].

(ii) The set $\mathbb{U}$ of control is convex and closed.

(iii) The right-hand side of the system (16) is bounded by a linear function of the state and control variables.

(iv) The integrand of the objective functional is convex with respect to $\mathbb{U}$.

(v) There exist constants $m_1, m_2 > 0$ and $\rho > 1$ such that the integrand $L(S, E, I, u_1, u_2)$ of the objective functional satisfies:

$$L(S, E, I, u_1, u_2) \geq m_2 + m_1(|u|^2)^{\rho/2}.$$

Therefore, using these conditions, we confirm that an optimal control exists.

3.2. Characterization of the Optimal Control

For deriving the necessary conditions for a control to be optimal, Pontryagin's Maximum Principle is applied. Based on this principle we transform our system into a minimization problem for the Hamiltonian $\mathbb{H}$, which is given by:

$$\mathbb{H} = A_1 S(t) + A_2 E(t) + A_3 I(t) - A_4 R(t) + A_5 V(t) + \frac{A_6}{2} u_1^2(t) + \frac{A_7}{2} u_2^2 + \sum_{i=1}^{5} \lambda_i k_i.$$

The right-hand terms of differential equations are represented by k_i corresponding to the i-th state variable.

Theorem 4. *Given an optimal control* $u^* = (u_1^*, u_2^*) \in \mathbb{U}$ *and corresponding variables* S, E, I, R, *and* V, *there exist adjoint variables* $\lambda_1, ..., \lambda_4$, *and* λ_5 *that must fulfill the following adjoint equations:*

$$\begin{aligned}
\dot{\lambda}_1 &= -A_1 + \lambda_1 \left(\frac{\beta I}{1 + \alpha I} + (\gamma_2 + \mu) \right) - \lambda_2 \left(\frac{\beta I}{1 + \alpha I} \right) - \lambda_5 \gamma_2, \\
\dot{\lambda}_2 &= -A_2 + \lambda_2 (\sigma + \mu + u_1) + \sigma \lambda_3 - u_1 \lambda_4, \\
\dot{\lambda}_3 &= -A_3 + \lambda_1 \left(\frac{\beta S}{(1 + \alpha I)^2} \right) - \lambda_2 \left(\frac{\beta S}{(1 + \alpha I)^2} \right) + \lambda_3 (\gamma_1 + \mu + u_2) - \lambda_4 (\gamma_1 + u_2)
\end{aligned}$$

$$\dot{\lambda}_4 = A_4 + \mu\lambda_4 + \gamma_2\lambda_5,$$
$$\dot{\lambda}_5 = A_5 + \mu\lambda_5,$$

following the transversality conditions:
$\lambda_1(T) = \lambda_2(T) = \lambda_3(T) = \lambda_4(T) = \lambda_5(T) = 0.$
Additionally, the optimal control $u_1^*(t)$ and $u_2^*(t)$ is characterized by:

$$u_1^*(t) = \min\left(1, \max\left(0, \frac{(\lambda_4 - \lambda_2)}{A_1}E\right)\right),$$
$$u_2^*(t) = \min\left(1, \max\left(0, \frac{(\lambda_4 - \lambda_3)}{A_2}I\right)\right).$$

Using Pontryagin's maximum principle adjoint equations and transversality conditions are derived. Specifically:

(i) **Adjoint Equations**:
The adjoint equations take the following form:

$$\dot{\lambda}_1 = -\frac{\partial H}{\partial S},$$
$$\dot{\lambda}_2 = -\frac{\partial H}{\partial E},$$
$$\dot{\lambda}_3 = -\frac{\partial H}{\partial I},$$
$$\dot{\lambda}_4 = -\frac{\partial H}{\partial R},$$
$$\dot{\lambda}_5 = -\frac{\partial H}{\partial V}.$$

(ii) **Optimal Control**:
The optimal control u_1^* and u_2^* can be determined from the optimality condition, which involves partially differentiating the Hamiltonian in terms of u_i to zero:

$$\frac{\partial H}{\partial u_1} = 0.$$
$$\frac{\partial H}{\partial u_2} = 0.$$

This yields:

$$-A_1u_1^* + (\lambda_4 - \lambda_2)(E) = 0.$$
$$-A_2u_2^* + (\lambda_4 - \lambda_3)(I) = 0.$$

Given the bounds on the control u_i specified by the set U, we express the optimal control u_1^* and u_2^* in the following form:

$$u_1^*(t) = \min\left(1, \max\left(0, \frac{(\lambda_4 - \lambda_2)}{A_1} E\right)\right),$$
$$u_2^*(t) = \min\left(1, \max\left(0, \frac{(\lambda_4 - \lambda_3)}{A_2} I\right)\right).$$

4. Numerical Simulation

To discuss the dynamics of disease spread and study the impact of both time delay and control strategies, we performed a numerical simulation of the solution trajectories of the model described in model (3), where classes (S,I,E) are independent of (R, V) and the adjoint model in Theorem (4.2). The parameter values model simulations are shown in Table 1.

Table 1. Parameter values of model (3).

Parameters	Value
Δ	0.87
β	0.01
α	0.1
μ	0.1
$\gamma_2 = \gamma_3$	0.1
γ_1	0.01
σ	0.2

The simulation of the model (3) illustrated in Figure 1, shows the dynamic behavior of the model (3) that approaches the extinction of the disease.

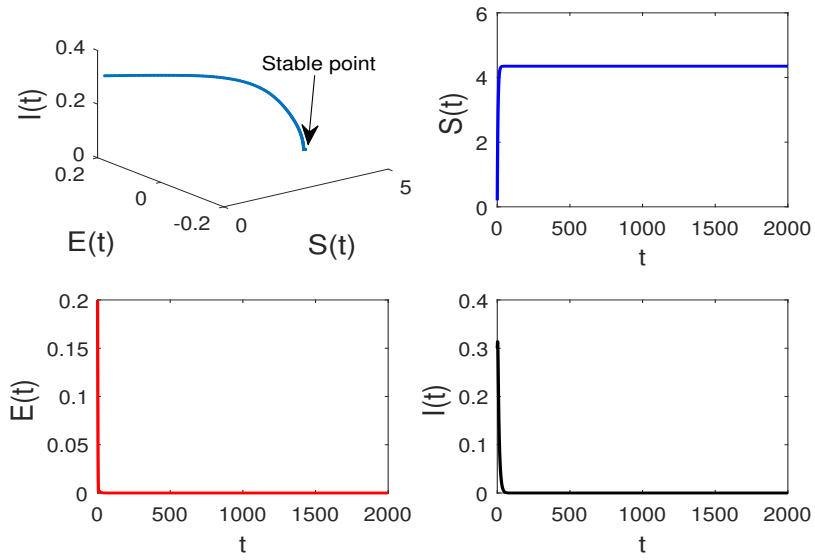

Figure 2: The trajectory of the system (3) using the parameters set in Table 1.

Now, we show the effect of increasing the infection rate on the dynamics of the model (3), by keeping the values of all parameters in Table 1 except the value of β we change it from 0.01 to 0.1 and $\tau < 18.5$, we get the solution of model 1, which tends to the endemic point; see Figure 2.

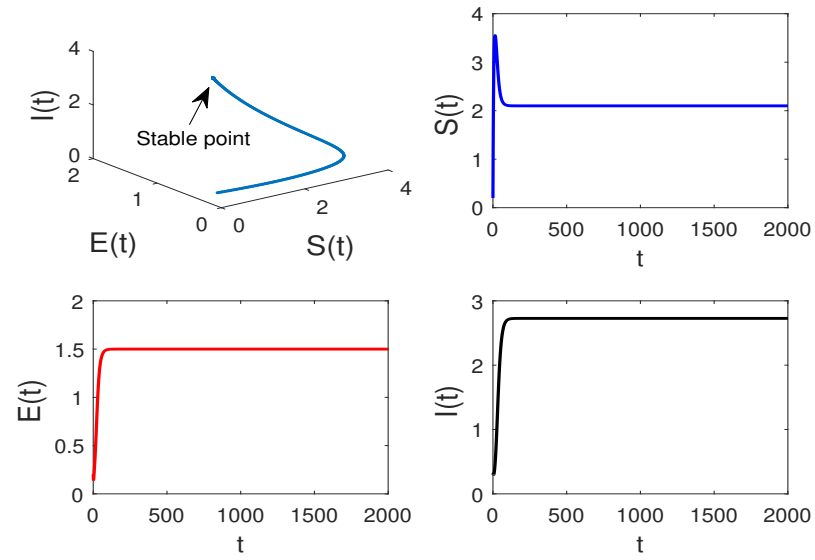

Figure 3: The trajectory of the system (3) using the parameters set in Table 1 with $\beta = 0.1$.

In addition, we also need to know the impact of time delay on the solution of the model (3). In Figure 3, if we choose the value of the parameter $\tau = \tau_0 = 18.5$. The figure tells us loss of stability of the endemic point and change of the system's behavior to the periodic state (occurring Hopf bifurcation). However, both figures (4) and (5) tell us the high periodic state when we increase the time delay such as $\tau = 20, 25$, respectively.

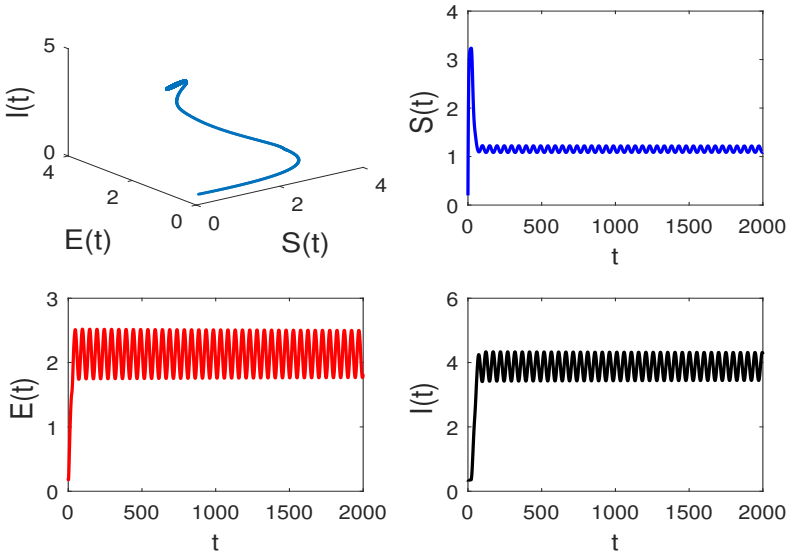

Figure 4: The trajectory of the model (3) using the parameters set in Table 1 with $\tau = 18.5$.

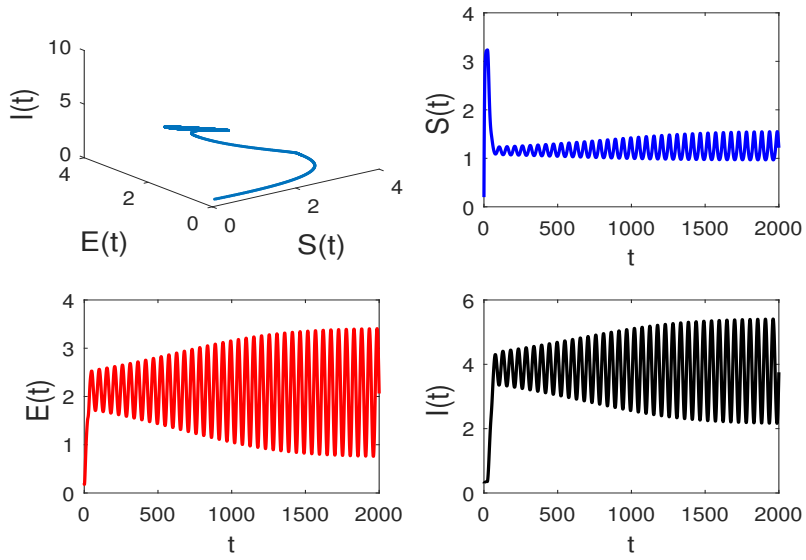

Figure 5: The trajectory of the model (3) using the parameters set in Table 1 with $\tau = 20$.

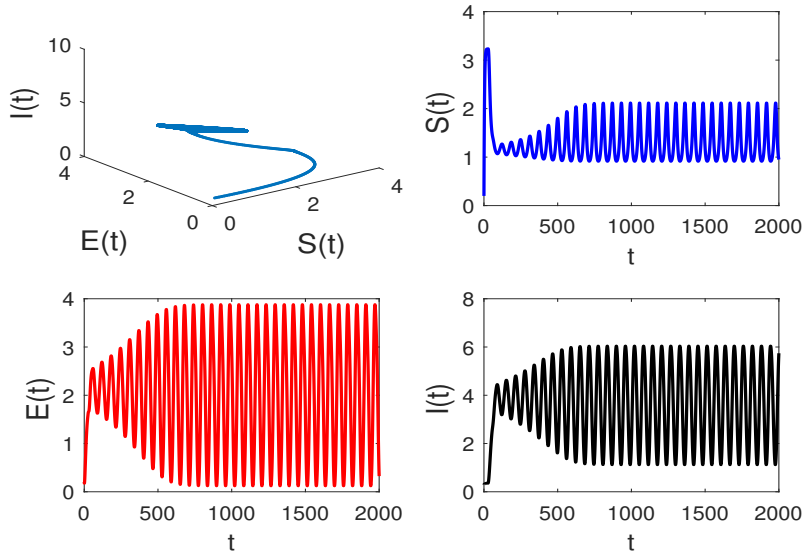

Figure 6: The trajectory of the system (3) using the parameters set in Table 1 with $\tau = 25$.

For the simulation analysis to the each control strategies are quarantine and treatment and represented by the parameters u_1 and u_2 respectively. The four scenarios for numerical simulation of the adjoint model are given below:

(i) Scenario A: There is no quarantine and no treatment available for the infected ($u_1 = u_2 = 0$).

(ii) Scenario B: Only quarantine is implemented ($u_1 \neq 0$, $u_2 = 0$).
(iii) Scenario C: Only treatment for the infected is provided ($u_1 = 0$, $u_2 \neq 0$).
(iv) Scenario D: A combination of both quarantine and treatment is implemented ($u_1 \neq 0$, $u_2 \neq 0$).

It is clear that, figure 6, shows that the impact of both scenarios (A) and (B) and this figure tell us when we increasing the quarantine rate (i.e. $u_1 \geq 0.5$) with keeping the other parameters in table 1 with $\beta = 0.1$ and $\tau < 18.5$, we get the dynamical behavior of system (3) tend towards disease extinction point.

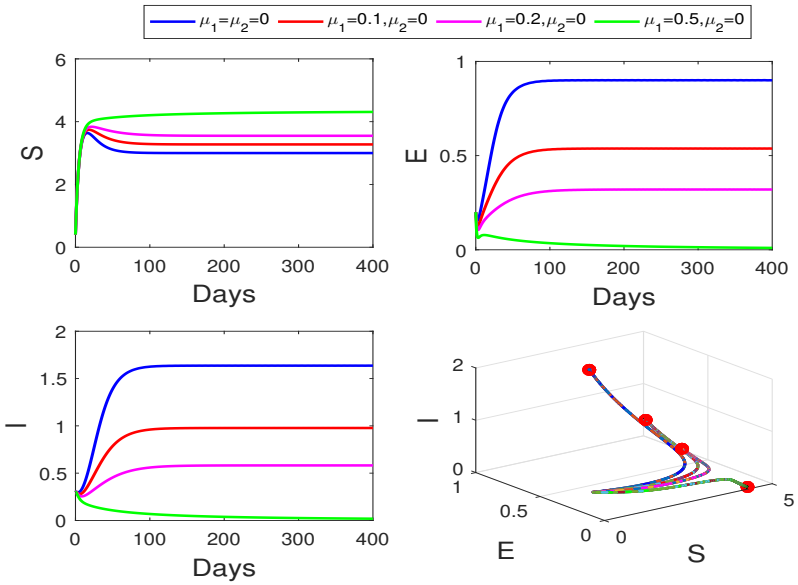

Figure 7: The trajectory of the model (3) with $\mu_2 = 0$ and different values of μ_1.

Thus, figure 7, presents that the impact of both scenarios (A) and (C) and this figure tell us when we increasing the treatment rate (i.e. $u_2 \geq 0.2$) with keeping the other parameters in table 1 with $\beta = 0.1$ and $\tau < 18.5$, we get the dynamical behavior of model (3) tend towards disease extinction point.

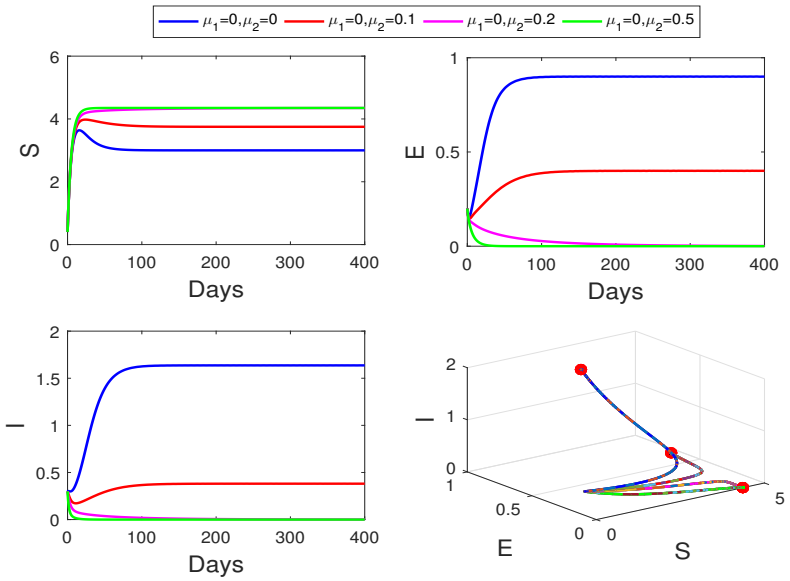

Figure 8: The trajectory of the system (3) with $\mu_1 = 0$ and different values of μ_2.

Finally, as depicted in Figure 7, scenario (D) leads to a more rapid progression toward disease extinction compared to scenarios (B) and (C), highlighting the enhanced effectiveness of the interventions assumed in this scenario.

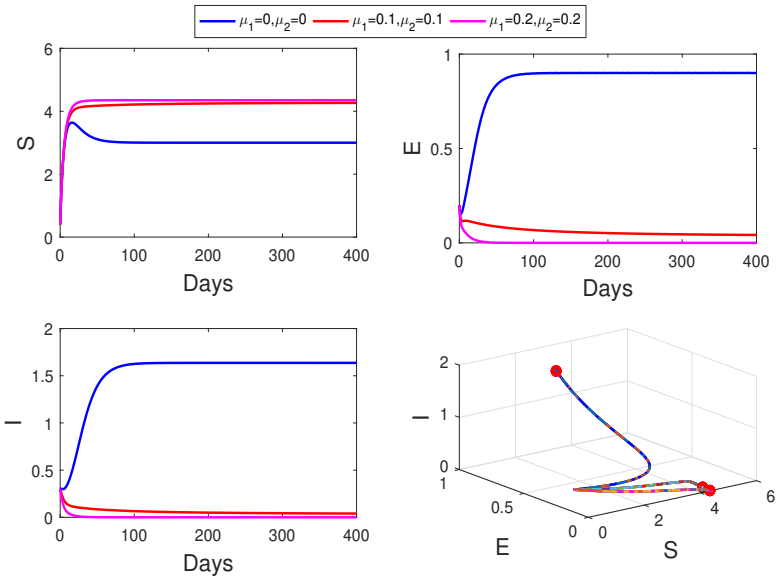

Figure 9: The trajectory of the system (3) with $\mu_1 = 0.2$ and $\mu_2 = 0.2$.

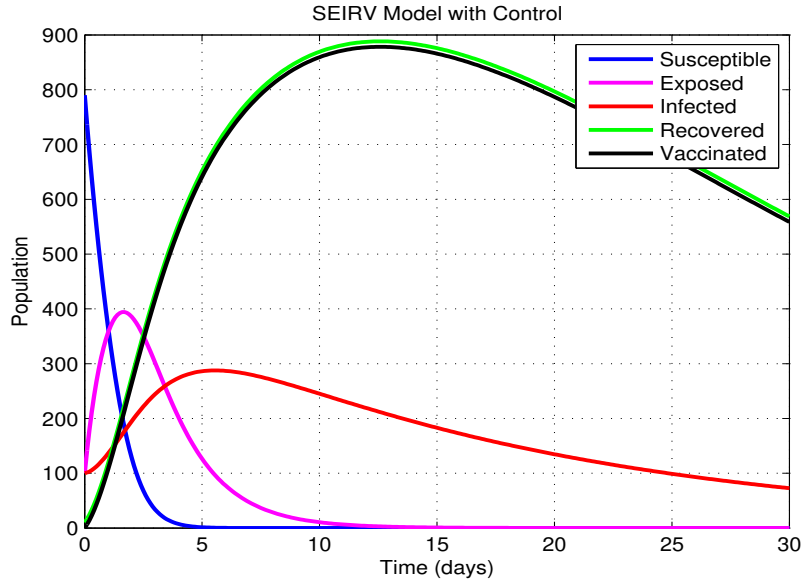

Figure 10: Control model (16).

The Figure 10, demonstrates the impact of optimal control strategies on disease progression. The interventions reduce the infection peak and overall number of cases, showcasing the effectiveness of control measures like vaccination, treatment, or public awareness.

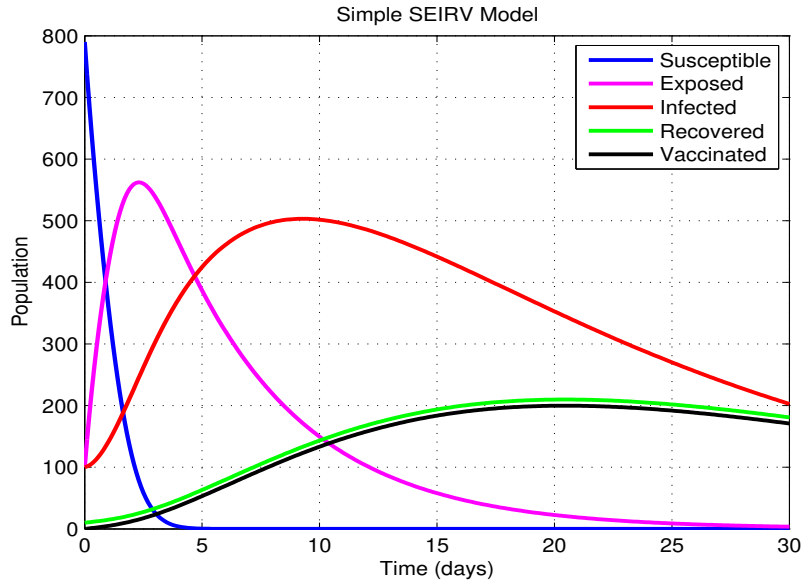

Figure 11: Without delay and control for model (16).

The Figure 11, illustrates the baseline epidemic dynamics without any delay or control interventions. The disease spreads naturally according to the model's parameters, showing typical infection peaks and declines.

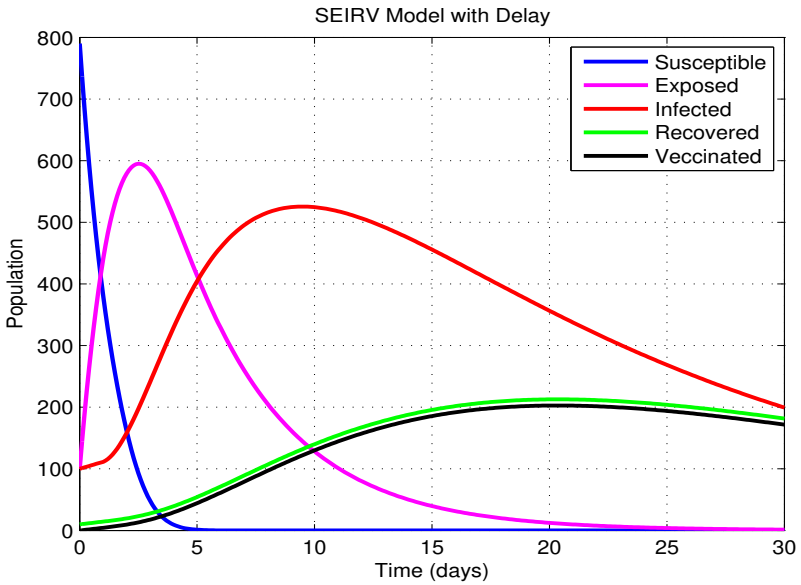

Figure 12: Without delay for model (16).

The Figure 12, reflects the influence of time delays in the epidemic model, such as delayed response to infection or incubation periods. The delay affects the timing and height of the epidemic peak, potentially causing oscillatory or more prolonged outbreaks.

5. Conclusion and Discussion

In recent paper, we formulate an epidemic model with time delay, consisting of five state variables and nine parameters. Based on the analytical results, two equilibrium points are identified: disease-free equilibrium and endemic equilibrium. The results show that the system exhibits stable behavior in disease-free equilibrium for all time delay values, given the parameter values presented in Table 1 (see Figure 2). However, when the infection rate increases, the system transitions to a stable endemic equilibrium, provided that the time delay is below 18.5 (see figure 3). This stability is lost when the time delay exceeds this threshold (see Figures 4-6). Furthermore, control variables are incorporated into the model, namely quarantine and treatment. Pontryagin's Maximum Principle is applied to solve the optimal control problem. Numerical simulations with specified weights indicate that the optimal strategy to control the disease spread is the combination of both control measures (see figure 7-9). Further direction is to apply the optimal control over a delayed system.

References

[1] Elham Taghizadeh and Ali Mohammad-Djafari. Seir modeling, simulation, parameter estimation, and their application for covid-19 epidemic prediction. *Phys. Sci. Forum*, 5(1):18, 2022.

[2] R. Paulo and J.P.Z. Zingano. A matlab code to compute reproduction numbers with applications to the covid-19 outbreak, 2020. arXiv:2006.13752.

[3] S. He, Y. Peng, and K. Sun. Seir modeling of the covid-19. *Nonlinear Dyn*, 101:1667–1680, 2020.

[4] J.P. Gleeson, T.B. Murphy, J.D. Brien, and D.J. Sullivan. A population-level seir model for covid-19 scenarios, 2020. Technical Note of the Irish Epidemiological Modelling Advisory Group to NPHET, Department of Health, Government of Ireland.

[5] Ahmed A. Mohsen, Hassan F. AL-Husseiny, and Raid Kamel Naji. The dynamics of corona virus pandemic disease model in the existence of a curfew strategy. *Journal of Interdisciplinary Mathematics*, 2022.

[6] Hassan F. AL-Husseiny, Nidhal F. Ali, and Ahmed A. Mohsen. The effect of epidemic disease outbreaks on the dynamic behavior of a prey-predator model with holling type ii functional response. *Commun. Math. Biol. Neurosci.*, 2021. Article ID 72.

[7] A. Acharya, S. Paul, M.A. Biswas, A. Mahata, S. Mukherjee, and B. Roy. Study of seirv epidemic model in imprecise environment. In *Advances in Intelligent System and Computing, ICMMCS*, pages 371–380. 2023.

[8] S. Paul, A. Acharya, M.A. Biswas, A. Mahata, S. Mukherjee, P.C. Mali, and B. Roy. The scenario of covid 19 pandemic in brazil using seir epidemic model. In *Advances in Intelligent System and Computing, ICMMCS*, pages 419–426. 2023.

[9] Ping Yan and Shengqiang Li. Seir epidimic model with delay. *ANZIAM J*, 48:119–134, 2006.

[10] Ahmed A. Mohsen and Raid Kamel Naji. Stability and bifurcation of a delay cancer model in the polluted environment. *Advances in Systems Science and Applications*, 22(3):1–17, 2022.

[11] Sajal and Fahad Mostafa. Seirv-holling type-ii: Implementing holling type functional response in covid-19 disease modeling. SSRN. https://ssrn.com/abstract=4953603.

[12] Animesh, Subrata Paul, Supriya Mukherjee, Meghadri Das, and Banamali Roy. Dynamics of caputo fractional order seirv epidimic model with optimal control and stability analysis. *International Journal of Applied and Computational Mathematics*, 8:28, 2022.

[13] Sarah A. Al-Sheikh. Modeling and analysis of seir epidimic model with limited resource of

treatment. *Global Journal of Science Frontier Research Mathematics and Decision Sciences*. Print ISSN: 0975-5896.

[14] Ahmed A. Mohsen and Raid Kamel Naji. Dynamical analysis within-host and between-host for hiv/aids with the application of optimal control strategy. *Iraqi Journal of Science*, 61(5):1173–1189, 2020.

[15] Oluwatosin Babasola, Oshinubi Kayode, Olumuyiwa James Peter, Faithful Chiagoziem Onwuegbuche, and Festus Abiodun Oguntolu. Time-delayed modelling of the covid-19 dynamics with a convex incidence rate. *Informatics in Medicine Unlocked*, 35:101124, 2022.

[16] S. Tipsri and W. Chinviriyasit. The effect of time delay on the dynamics of an seir model with nonlinear incidence. *Chaos Solitons Fractals*, 75:153–172, 2015.

[17] W.H. Fleming and R.W. Rishel. *Deterministic and Stochastic Optimal Control*. Springer, New York, NY, USA, 1975.

[18] D.L. Lukes. *Differential Equations: Classical to Controlled*. Academic Press, New York, 1982.